Excitation Energy Transfer Studies of the Proximity between Tropomyosin and Actin in Reconstituted Skeletal Muscle Thin Filaments†

Terence Tao,* Mark Lamkin, and Sherwin S. Lehrer

Appendix: Computer Simulation Study on the Extent of Energy Transfer from a Single Tm-Bound Donor to Multiple Actin-Bound Acceptors

Terence Tao* and Edward P. Morris

ABSTRACT: Fluorescence excitation energy transfer studies were carried out to measure the distance between labels attached at specific sites in tropomyosin and in actin. Rabbit skeletal $\alpha\alpha$-tropomyosin was donor labeled at cysteine-190 with *N*-(iodoacetyl)-*N'*-(1-naphthyl-5-sulfo)ethylenediamine (1,5-IAEDANS). Actin was acceptor labeled at two different sites with two different reagents: covalently at cysteine-373 with *N*-[4-[[4-(dimethylamino)phenyl]azo]phenyl]maleimide (DAB-Mal) and noncovalently at the nucleotide binding site with 2'(3')-*O*-(2,4,6-trinitrophenyl)adenosine 5'-diphosphate (TNP-ADP). Under the assumption that the orientation factor κ^2 is $^2/_3$, the critical transfer distance was calculated to be ~40 Å for both donor–acceptor pairs. Energy transfer efficiencies were obtained by measuring the decrease in donor fluorescence lifetime when donor-labeled tropomyosin was bound to acceptor-labeled F-actins. In the absence of troponin, apparent distances of ~46 Å were obtained for both donor–acceptor pairs. In the presence of troponin, there was no detectable difference in the energy transfer efficiency when calcium ions were present or absent. A computer simulation study showed that a movement of tropomyosin in the grooves of actin would produce no net change in the energy transfer efficiency if the acceptor is located in a certain region on the surface of actin. Thus, further information on the locations of the acceptors on actin is required before one can determine if these findings are contrary to the proposal that tropomyosin undergoes a calcium-induced movement.

It is now well established that the regulatory muscle proteins tropomyosin (Tm)[1] and troponin (Tn) act in concert to regulate the contraction of mammalian striated muscle and that contraction is initiated when calcium ions released from the sarcoplasmic reticulum are bound to troponin (Ebashi & Endo, 1968). The mechanism of this regulation process is still not clear. One hypothesis is the "steric blocking model", which postulates that in the relaxed state (absence of Ca^{2+}), Tm assumes a position that blocks the interaction between actin and the myosin cross bridges, while in the contracting state Ca^{2+} acting on Tn induces Tm to move to a position that clears the myosin–actin interaction site, allowing myosin–actin interaction to take place (Huxley, 1972; Haselgrove, 1972; Parry & Squire, 1973).

Central to the steric blocking model is the premise that there is a calcium-induced movement of Tm in the thin filament. X-ray diffraction studies on intact muscle fibers (Huxley, 1971; Vibert et al., 1972) revealed characteristic changes in layer line intensities depending on whether the muscle was in a relaxed or contracting state; modeling studies showed that these intensity changes could be accounted for by a movement of Tm in the actin grooves (Haselgrove, 1972; Parry & Squire, 1973). Later electron microscopy studies on paracrystals of reconstituted thin filaments yielded similar conclusions (Wakabayashi et al., 1975; Gillis & O'Brien, 1975). Thus, there is strong structural evidence for the existence of this Tm movement. It is important, however, to detect this Tm movement in vitro in order to characterize the calcium dependence and dynamics of this process. The technique of singlet–singlet excitation energy transfer (Stryer, 1978; Fairclough & Cantor, 1978) is well suited to approach this problem. However, previous studies have yielded disparate results. Using nonspecific labeling reagents, Poo & Hartshorne (1976) reported that the extent of energy transfer from Tm-bound donors to actin-bound acceptors was calcium dependent. Using sulfhydryl-specific labeling reagents, however, Lin & Dowben (1983) found no calcium-dependent changes in energy transfer between a Tm-bound donor and an actin-bound acceptor.

In order to shed further light on this question, we have carried out detailed energy transfer studies on a well-characterized system composed of specifically labeled Tm and actin. Rabbit skeletal $\alpha\alpha$Tm was specifically labeled at Cys-190 with the fluorescent probe 1,5-IAEDANS. Actin was labeled with acceptors at two specific locations: Cys-373 with

† From the Department of Muscle Research, Boston Biomedical Research Institute, Boston, Massachusetts 02114, and the Department of Neurology, Harvard Medical School, Boston, Massachusetts 02115. *Received August 20, 1982; revised manuscript received December 21, 1982.* Supported by Grants AM-21673 and HL-22461 from the National Institutes of Health and by the Muscular Dystrophy Association. A preliminary account of this work was presented at the Seventh International Biophysics Congress, Mexico City, Mexico, Aug 1981.

* Address correspondence to this author at the Department of Muscle Research, Boston Biomedical Research Institute, 20 Staniford Street, Boston, MA 02114.

[1] Abbreviations: Tm, tropomyosin; Tn, troponin; S1, myosin subfragment 1; 1,5-IAEDANS, *N*-(iodoacetyl)-*N'*-(1-naphthyl-5-sulfo)-ethylenediamine; DAB-Mal, *N*-[4-[[4-(dimethylamino)phenyl]azo]-phenyl]maleimide; TNP-ATP and TNP-ADP, 2'(3')-*O*-(2,4,6-trinitrophenyl)adenosine 5'-triphosphate and 5'-diphosphate, respectively; Tm*, 1,5-IAEDANS-labeled $\alpha\alpha$Tm; DAB-F-actin, DAB-Mal-labeled F-actin; DAB-ME, adduct of β-mercaptoethanol and DAB-Mal; TNP-F-actin, TNP-ADP-labeled F-actin; Hepes, *N*-(2-hydroxyethyl)piperazine-*N'*-2-ethanesulfonic acid; Nbs_2, 5,5'-dithiobis(2-nitrobenzoate); GdmCl, guanidinium chloride; EGTA, ethylene glycol bis(β-aminoethyl ether)-*N,N,N',N'*-tetraacetic acid; MalNEt, *N*-ethylmaleimide.

0006-2960/83/0422-3059$01.50/0

the nonfluorescent chromophore DAB-Mal and the nucleotide binding site with the chromophoric nucleotide analogue TNP-ADP. The critical transfer distance was calculated to be about 40 Å for both donor–acceptor systems. When the donor fluorescence lifetime was monitored, transfer efficiencies of ~30% were obtained for both systems, corresponding to an apparent separation distance of ~46 Å. When Tn was added to either system, no calcium-dependent change in the transfer efficiency was detectable, suggesting that no calcium-dependent Tm movement was present. A computer simulation study, however, showed that for acceptors located within a certain region on the surface of actin, the extent of energy transfer was insensitive to the movement of Tm. Thus, the apparent conflict between our results and results from structural studies can be resolved if both acceptor-labeling sites in actin are located within this region. Further information on the location of these labeling sites in actin will be needed before unambiguous interpretation of our results can be made.

Experimental Procedures

Materials. 1,5-IAEDANS was from Aldrich. TNP-ATP and DAB-Mal were from Molecular Probes (Junction City, OR). Other common materials used for buffers and routine analysis were from Sigma.

Protein Preparations. Preparation of $\alpha\alpha$Tm, Tn, actin, and myosin S1, as well as 1,5-IAEDANS labeling of $\alpha\alpha$Tm, was described in the preceding paper (Lamkin et al., 1983).

DAB-labeled actin was prepared by incubating G-actin (3 mg/mL) with a 2-fold molar excess of DAB-Mal (added from a 4 mM dimethylformamide stock solution) in G buffer (2 mM Hepes, 0.2 mM $CaCl_2$, and 0.2 mM ATP, pH 7.5) at 4 °C for 24 h. The reaction was quenched by excess dithiothreitol, and excess reagents were removed by dialysis against G buffer. For one DAB-G-actin preparation, excess reagent was removed by Sephadex G-25 gel chromatography as well as by dialysis. The labeling ratio (defined as moles of label per mole of protein) of the chromatographed DAB-G-actin decreased by no more than 5% compared to the dialyzed preparation. Also, a dialyzed sample was subsequently subjected to gel chromatography. Again, the labeling ratio did not decrease by more than 5%. DAB-F-actin was obtained by polymerizing DAB-G-actin in 50 mM NaCl and 2 mM $MgCl_2$.

TNP-F-actin was prepared as follows: the ATP in a solution of G-actin (3 mg/mL) was continuously replaced by 0.1 mM TNP-ATP by using a Millipore "immersible molecular separator". The resultant TNP-G-actin was polymerized to form TNP-F-actin by the addition of 50 mM NaCl and 2 mM $MgCl_2$.

In order to ascertain whether DAB-Mal reacts with G-actin at the same site as MalNEt, G-actin was first partially labeled with MalNEt, followed by DAB-Mal labeling. Conversely, G-actin was first partially labeled with DAB-Mal, followed by complete MalNEt labeling. Partial MalNEt labeling was carried out by incubating G-actin (3 mg/mL) with an equimolar amount of MalNEt at 25 °C, as described by Elzinga & Collins (1975). After ~1 h the reaction was quenched with excess dithiothreitol and dialyzed against G buffer. The amount of MalNEt that reacted was calculated from the decrease in absorbance at 310 nm by using $\Delta\epsilon_{310}$(MalNEt) = 580 M^{-1} cm^{-1} (Lehrer et al., 1972). Complete MalNEt labeling was carried out by incubating DAB-G-actin (2.8 mg/mL) with a 2.5-fold molar excess of MalNEt. The reaction was followed by monitoring the absorbance at 310 nm, until no further decrease in absorbance was discernible. The amount of MalNEt that reacted was again calculated from ΔA_{310}.

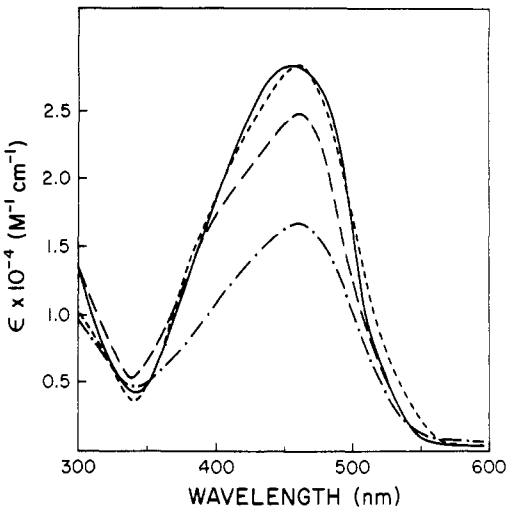

FIGURE 1: Absorption spectra of DAB derivatives (pH 7.5): DAB-F-actin in 4 M GdmCl (—), DAB-ME in 4 M GdmCl (- - -), DAB-F-actin in the absence of GdmCl (– –), and DAB-ME in the absence of GdmCl (- · -).

The labeling ratio of TNP-F-actin was determined by first sedimenting a sample at 80000*g* for 3 h, then the pellets were resuspended in G buffer, and the absorbances at 408 and 290 nm were measured. The labeling ratio n_L was obtained from

$$n_L = [\text{TNP-ADP}]/[\text{actin}]$$

$$[\text{TNP-ADP}] = A_{408}/\epsilon_{408}(\text{TNP})$$

$$[\text{actin}] = \frac{A_{290} - [\text{TNP-ADP}]\epsilon_{290}(\text{TNP})}{E_{290}(\text{actin})} M_r(\text{actin})$$

by using extinction coefficients ϵ_{408}(TNP) = 26 400 M^{-1} cm^{-1} and ϵ_{290}(TNP) = 8000 M^{-1} cm^{-1} (Hiratsuka & Uchida, 1973), specific absorbance E_{290}(actin) = 0.63 $(mg/mL)^{-1}$ cm^{-1} (Lehrer & Kerwar, 1972), and molecular weight for actin = 42 300 (Elzinga et al., 1973). Similarly, n_L for DAB-G-actin was determined for the absorbances at 460 and 290 nm by using extinction coefficients ϵ_{460}(DAB) = 24 800 M^{-1} cm^{-1} and ϵ_{290}(DAB) = 8400 cm^{-1} cm^{-1} (see next section). Typical labeling ratios were 1.0 for TNP-F-actin and 0.92 for DAB-G-actin. For some of the DAB-G-actin preparations, the amount of actin was also determined by the Lowry method with unlabeled Tm as standards. Within an experimental error of 8%, the resultant labeling ratios were identical with those obtained by the spectrophotometric method.

Extinction Coefficient Determination for the F-Actin-Bound DAB Moiety. A known amount of DAB-Mal was reacted with a 10-fold molar excess of β-mercaptoethanol. The absorption spectra of the resultant adduct (DAB-ME) were taken in the absence and presence of 4 M GdmCl (Figure 1). Assuming that the extinction coefficients of DAB-F-actin and DAB-ME are identical under denaturing conditions, we have

$$\frac{\epsilon(\text{DAB-F-actin})_{-\text{GdmCl}}}{\epsilon(\text{DAB-F-actin})_{+\text{GdmCl}}} = \frac{\epsilon(\text{DAB-F-actin})_{-\text{GdmCl}}}{\epsilon(\text{DAB-ME})_{+\text{GdmCl}}} = \frac{A(\text{DAB-F-actin})_{-\text{GdmCl}}}{A(\text{DAB-F-actin})_{+\text{GdmCl}}}$$

ϵ(DAB-ME)$_{+\text{GdmCl}}$ and the right-most ratio of absorbances could be obtained from the absorption spectra in Figure 1. Thus, ϵ(DAB-F-actin)$_{-\text{GdmCl}}$ at any wavelength could readily be calculated.

Other Methods. Spectrophotometry, spectrofluorometry, fluorescence lifetime measurements, binding assays, and AT-Pase measurements were described in the preceding paper

Table I: ATPase Activities for Donor- and Acceptor-Labeled Muscle Proteins[a]

samples	ATPase [mol of ATP (mol of S1)$^{-1}$ s^{-1}]
S1	0.031
S1 + F-actin	0.154
S1 + Tm-F-actin	0.077
S1 + Tn-Tm-F-actin + Ca^{2+}	0.096
S1 + Tn-Tm-F-actin + EGTA	0.032
S1	0.041
S1 + DAB-F-actin	0.099
S1 + Tm*-DAB-F-actin	0.055
S1 + Tn-Tm*-DAB-F-actin + Ca^{2+}	0.082
S1 + Tn-Tm*-DAB-F-actin + EGTA	0.017
S1	0.036
S1 + TNP-F-actin	0.089
S1 + Tm*-TNP-F-actin	0.065
S1 + Tn-Tm*-TNP-F-actin + Ca^{2+}	0.108
S1 + Tn-Tm*-TNP-F-actin + EGTA	0.032

[a] ATP hydrolysis rates were obtained from pH-stat traces. [S1] = 2.2 μM, [F-actin] = 1.3 μM, [Tm] = 0.27 μM, [Tn] = 0.3 μM, [Ca^{2+}] = 50 μM, and [EGTA] = 1.3 mM, in 0.03 M NaCl and 5 mM $MgCl_2$, 23 °C, pH 7.9.

(Lamkin et al., 1983). The quantum yield of Tm* was obtained by comparing its integrated corrected fluorescence spectrum with that of quinine sulfate in 0.1 N H_2SO_4, whose quantum yield was taken to be 0.70 (Scott et al., 1970). Overlap integrals were obtained by numerical integration at 5-nm intervals by using Simpson's rule.

Results

Specificity and Effects of Protein Labeling. Evidence that the AEDANS label in Tm* (1,5-IAEDANS-labeled αα Tm) is specifically attached at Cys-190 was presented in the preceding paper (Lamkin et al., 1983), as was our finding that the structure and function of Tm* is similar to that of unlabeled Tm.

Although the location at which DAB-Mal labels actin was not directly determined, it is presumed to be cysteine-373 because a large amount of work had reported that this residue is the most reactive toward sulfhydryl reagents (Lusty & Fasold, 1969; Bridgen, 1972; Lehrer et al., 1972; Elzinga & Collins, 1975; Bender et al., 1976; Lin, 1978; Tao & Cho, 1979). We have partially labeled a sample of G-actin with MalNEt using conditions similar to what Elzinga & Collins (1975) used, followed by DAB-Mal labeling using conditions described under Experimental Procedures. The resultant labeling ratios were such that [MalNEt]/[actin] + [DAB]/[actin] = 0.63 + 0.28 = 0.91. Conversely, when G-actin was first partially labeled with DAB-Mal, followed by full labeling with MalNEt, we obtained [DAB]/[actin] + [MalNEt]/[actin] = 0.40 + 0.67 = 1.07. These results strongly suggest that DAB-Mal labels G-actin at the same site as MalNEt. Since Elzinga & Collins (1975) found that MalNEt labels Cys-373 of G-actin with 85–90% specificity (using radioactive MalNEt and peptide analysis methods), it is reasonable to assume that DAB-Mal labels Cys-373 with roughly the same specificity.

On the basis of the stoichiometry and its similarity in structure to ADP, it is also reasonable to assume that TNP-ADP replaces ADP at the nucleotide binding site of actin.

We found that the ability of DAB-F-actin and TNP-F-actin to stimulate the Mg^{2+}-ATPase activity of myosin S1 to be impaired but not abolished (Table I). Nonetheless, the ATPase activity of reconstituted systems composed of S1, Tn, Tm*, and acceptor-labeled F-actin exhibited marked Ca^{2+} sensitivity; in the absence of Ca^{2+} (in the presence of EGTA) the ATPase activity drops to the same level as that of S1 alone; in the presence of Ca^{2+} the ATPase activity is at least as high as that of the system reconstituted from unlabeled proteins (Table I). These results show that although the labeled proteins exhibit somewhat modified behavior, they seem to retain their essential property of being able to participate in the calcium regulation process.

Energy Transfer Results. The fluorescence decay of Tm* in the presence of DAB-G-actin was identical with that in the presence of unlabeled G-actin (not shown). This could be expected since Tm is not known to interact with G-actin. When the ionic strengths of these samples were raised to polymerize the actins, Tm*–DAB-F-actin distinctly exhibited a shorter decay component when compared to Tm*–F-actin (Figure 2), undoubtedly due to energy transfer from the AEDANS moiety to the DAB moiety. The decay curves for both Tm*–F-actin and Tm*–DAB-F-actin were well fitted by sums of two exponentials (Figure 2). The energy transfer efficiency E was calculated by using

$$E = 1 - \tau_{da}/\tau_{d}$$

where τ_d, the donor lifetime in the absence of acceptors, was taken as the lifetime of the major component of Tm*–F-actin,

Table II: Fluorescence Decay and Energy Transfer Parameters for Donor-Labeled Tm and Acceptor-Labeled F-Actins[a]

samples	A_1	τ_1 (ns)	A_2	τ_2 (ns)	E	R' (Å)
Tm*	1.000	13.55[b]				
Tm*-F-actin	0.976	13.32	0.024	25.52		
Tm*-DAB-F-actin	0.826	9.24	0.174	16.38	0.306	45.7
Tn-Tm*-F-actin + Ca^{2+}[c]	0.786	13.39	0.214	20.83		
Tn-Tm*-DAB-F-actin + Ca^{2+}[d]	0.770	7.03	0.229	14.68	0.475	40.6
Tn-Tm*-F-actin + EGTA	0.872	13.85	0.128	22.83		
Tn-Tm*-DAB-F-actin + EGTA	0.885	7.69	0.115	16.98	0.445	41.4
Tm*-F-actin	0.900	12.89	0.100	21.22		
Tm*-TNP-F-actin	0.607	9.42	0.393	16.05	0.269	46.6
Tn-Tm*-F-actin + Ca^{2+}	0.780	13.00	0.220	20.47		
Tn-Tm*-TNP-F-actin + Ca^{2+}	0.658	9.19	0.342	17.58	0.293	45.6
Tn-Tm*-F-actin + EGTA	0.861	13.67	0.139	22.37		
Tn-Tm*-TNP-F-actin + EGTA	0.631	9.03	0.369	17.34	0.338	44.1

[a] A_1 and A_2 are the amplitudes of the major and minor decay components, respectively; τ_1 and τ_2 are lifetimes of the major and minor decay components, respectively. Values were obtained from method of moments analysis. E is the energy transfer efficiency, and R' is the apparent distance. Typical concentrations were [Tm*] = 2.0 μM, [F-actin] = 19 μM, [Tn] = 3.0 μM, [Ca^{2+}] = 0.1 mM, and [EGTA] = 0.3 mM, in 10 mM Hepes, 50 mM NaCl, and 2 mM $MgCl_2$, pH 7.5, 25 °C. [b] The mean of four determinations on four different Tm* preparations, with a standard deviation of 0.08 ns. [c] Three-exponential analysis yielded the following parameters: $A_1 = 0.652$, $\tau_1 = 12.51$ ns, $A_2 = 0.348$, $\tau_2 = 19.24$ ns, $A_3 = -4.3 \times 10^{-11}$, and $\tau_3 = 175.30$ ns. [d] Three-exponential analysis yielded $A_1 = 0.803$, $\tau_1 = 7.74$ ns, $A_2 = 0.197$, $\tau_2 = 15.13$ ns, $A_3 = -4.87 \times 10^{-5}$, and $\tau_3 = 48.33$ ns.

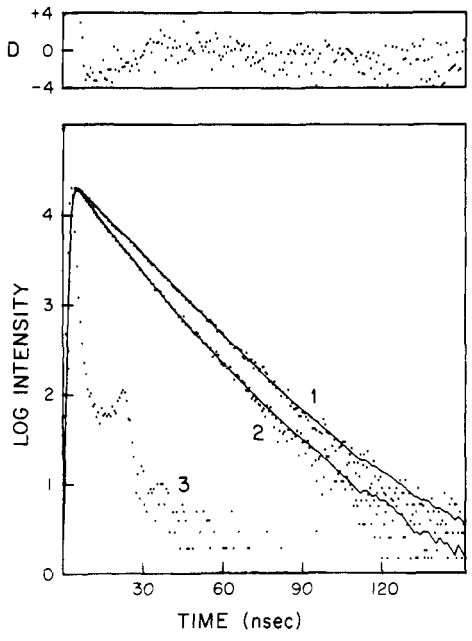

FIGURE 2: Fluorescence decay curves of Tm*–F-actin (curve 1) and Tm*–DAB-F-actin (curve 2) are well represented by sums of two exponentials (see Table II for decay parameters). Dots are experimental points (F_e); solid lines are the calculated fits (F_c). Top panel shows the deviation function for Tm*–DAB-F-actin, defined as $D = (F_c - F_e)/F_e^{1/2}$. Curve 3 is the excitation curve.

viz., 13.32 ns (Table II), and τ_{da}, the donor lifetime in the presence of acceptors, was taken as the lifetime of the major component of Tm*–DAB-F-actin, viz., 9.24 ns. Whence, we obtained $E = 0.306$ for energy transfer between Tm* and DAB-F-actin.

Energy transfer measurements were carried out on the following additional systems: Tn–Tm*–DAB-F-actin in the presence and absence of Ca^{2+}, Tm*–TNP-F-actin, and Tn–Tm*–TNP-F-actin in the presence and absence of Ca^{2+}. For all systems, energy transfer efficiencies were obtained in a manner similar to that for Tm*–DAB-F-actin: the lifetimes of the major decay component of samples containing Tm* complexed with unlabeled actins were taken to be τ_d, while the lifetimes of the major decay component of samples containing Tm* complexed with acceptor-labeled actins were taken to be τ_{da}. The results are shown in Table II.

Apparent distances were obtained by using equations derived by Forster (1959). Critical transfer distances (R_0) (Å) were calculated by using

$$R_0 = [(8.79 \times 10^{-5})\kappa^2 n^{-4} Q J]^{1/6}$$

Q is the quantum yield of Tm*, which we determined to be 0.53; n is the refractive index of the medium, taken to be 1.4 (Fairclough & Cantor, 1978); κ^2 is the orientation factor; although κ^2 can in principle take on any value in the range 0–4, we assume for the time being that $\kappa^2 = {}^2/_3$; J, the overlap integral, is given by

$$J = \int F(\lambda)\epsilon(\lambda)\lambda^4 \, d\lambda / \int F(\lambda) \, d\lambda$$

where $F(\lambda)$ is the corrected fluorescence spectrum of Tm* and $\epsilon(\lambda)$ is the absorption spectrum of either DAB-F-actin or TNP-F-actin. By numerical integration at 5-nm intervals, we obtained $J = 5.0158 \times 10^{14}$ cm^{-1} M^{-1} nm^4 for the Tm*–DAB-F-actin system and $J = 4.6492 \times 10^{14}$ cm^{-1} M^{-1} nm^4 for the Tm*–TNP-F-actin system. From these values, we obtained $R_0 = 39.9$ Å for Tm*–DAB-F-actin and $R_0 = 39.4$ Å for Tm*–TNP-F-actin. Finally, apparent distances R' were calculated by using

$$R' = R_0(E^{-1} - 1)^{1/6}$$

and are presented in Table II. We should point out that the meaning of the apparent distance R' is not well-defined because the geometry is such that each Tm-bound donor can transfer excitation to several actin-bound acceptors simultaneously (see footnote *a* in Table IV for more precise definition). In this respect, the quantity is used here merely as a rough indication of proximity and of changes therein.

Polarization Measurements. In order to obtain information on the extent of segmental motion that the AEDANS label can undergo, the steady-state fluorescence anisotropy (A) of a Tm* sample (with a labeling ratio of 1.2) was measured as a function of temperature from 4 to 25 °C. From a modified Perrin plot (not shown) the limiting anisotropy A_1 for Tm* was determined to be 0.09. In contrast, the intrinsic limiting anisotropy A_0 for the AEDANS moiety is known to be 0.32 [Hudson & Weber (1973), quoted in Wu et al. (1976)]. This suggests that the AEDANS label in Tm* undergoes substantial rapid reorientation [see also Wahl et al. (1978)] and that a certain amount of dynamic averaging can be carried out to limit the range of values that κ^2 can take on (Dale & Eisinger, 1975). According to Kawato et al. (1977), the rapid depolarization can be attributed to rapid reorientation of the label within the volume of a cone of semiangle θ, where

$$\begin{aligned}(\cos\theta)(1 + \cos\theta) &= 2(A_1/A_0)^{1/2} \\ &= 2(0.28)^{1/2} \end{aligned} \quad (1)$$

Solving eq 1 yielded $\theta = 49.8°$. In a formalism presented by Stryer (1978), a quantity α was defined in the following manner:

$$R = \alpha R' = (1.5\kappa^2)^{1/6} R' \quad (2)$$

where R' is an apparent distance calculated under the assumption that $\kappa^2 = {}^2/_3$ and R is the actual distance. Given θ, the range of values that α, and also R, can take on can be obtained from Figure 1 in Stryer (1978) (note that the acceptor is assumed to have no rotational freedom). Applying this formalism here, we obtained $0.75 \leq \alpha \leq 1.28$. Considering, for example, the Tm*–DAB-F-actin system (for which $R' = 45.7$ Å) the range of R is given by 34.2 Å $\leq R \leq$ 58.5 Å. The range of R for any other system can be similarly calculated with eq 2.

Discussion

Uncertainties in the Transfer Efficiency Determinations. In order to determine the transfer efficiency, it was necessary to obtain τ_d and τ_{da}, the donor lifetimes in the absence and presence of acceptor, respectively. We had assumed that τ_d and τ_{da} could be taken as the major component lifetimes of samples containing Tm* complexed with unlabeled F-actin and of samples containing Tm* complexed with acceptor-labeled F-actin, respectively. In what follows, we discuss the validity of these assumptions.

The fluorescence decay of Tm*–F-actin, for example, contains a major component of lifetime $\tau_1 = 13.32$ ns and a minor component of lifetime $\tau_2 = 25.52$ ns (Figure 2 and Table II). On the basis of both lifetime and acrylamide quenching studies, we had previously ascribed the major component to a class of AEDANS labels that lie in an exposed hydrophilic environment on the surface of the Tm* molecule and the minor component to AEDANS labels that lie in a buried hydrophobic environment at the actin–Tm* interaction interface (Lamkin et al., 1983). The fluorescence decay of Tm*–DAB-F-actin also contains a major and a minor component of, in this case, lifetimes $\tau_1 = 9.24$ ns and $\tau_2 = 16.38$ ns, respectively (Figure

2 and Table II). Presumably, the same two classes of AEDANS labels are present in Tm*–DAB-F-actin, giving rise to the two decay components. It may also be presumed that the decrease in both τ_1 and τ_2 is due to energy transfer from the Tm-bound AEDANS moiety to the actin-bound DAB moiety. Thus, in principle, we could choose either the τ_1's, or the τ_2's as τ_d and τ_{da}. In practice, we took τ_1 for Tm*–F-actin as τ_d, and τ_1 for Tm*–DAB-F-actin as τ_{da} because the lifetimes of the major decay components are more accurately determined than those of the minor decay components. Since the results for the other samples (Table II) are similar to those for Tm*–F-actin and Tm*-DAB-F-actin, the analyses are therefore also similar.

We have attempted to examine the errors involved in our transfer efficiency determinations. The mean of τ_1 for six different samples of Tm*–F-actin is 13.35 ns, with a standard deviation of 0.37 ns. On the basis of its reproducibility and its similarity to the lifetime of uncomplexed Tm* (13.55 ns), we feel that τ_d is relatively well determined, with an estimated uncertainty of only 3%. τ_{da}, on the other hand, may not be as well determined for the following reason: the analyses of the decay curves for samples containing Tm* and acceptor-labeled F-actins may be complicated by the presence of a certain amount of uncomplexed Tm*, which would give rise to an additional 13.55-ns lifetime decay component. We found, however, that two exponentials fitted these decay curves reasonably well (Figure 2). Also, three-exponential analyses of certain decay curves yielded a third component of negligible amplitude. These findings suggest that the amount of uncomplexed Tm* is not large enough to be detectable. Our cosedimentation binding assays show that the amount of uncomplexed Tm* is indeed small (5–10%), especially for those samples that contain Tn as well as F-actin. Judging from the quality of the fit (Figure 2), we feel that the determinations of τ_1 for samples containing Tm* and acceptor-labeled F-actins (i.e., τ_{da}) cannot be in error by more than 20%. When 3% is taken as the estimated uncertainty in τ_d and 20% as the estimated uncertainty in τ_{da}, the uncertainty in the transfer efficiency E amounts to 18%, corresponding to an uncertainty of 7% in the calculated apparent distance R'.

Orientation Factor κ^2. As is well-known, distance determinations using energy transfer measurements are subject to the uncertainty in the value of the orientation factor κ^2. In principle, κ^2 can vary between 0 and 4. In practice, any independent rotational mobility of the donor and/or acceptor with respect to the macromolecule serves to restrict the range of values that κ^2 can take on (Dale & Eisinger, 1975). In the limit of complete rotational freedom for both the donor and the acceptor, κ^2 averages to the value $^2/_3$. For this study, we could expect considerable dynamic averaging to take place, because the orientation of the AEDANS label in labeled skeletal Tm appears to be rapidly randomized due to both reorientation and energy transfer between adjacent labels (Wahl et al., 1978). By use of our measured limiting anisotropy for our preparations of Tm*, the dynamic averaging method yielded an uncertainty of $\sim$28% in the value of R', where the acceptor orientation was assumed to be fixed (see Results). We can expect this uncertainty to be smaller for samples containing Tm* and DAB-F-actin because labels attached at Cys-373 of actin appear to have some independent rotational mobility (Tao, 1978) as well.

Our results show that there is no calcium-dependent change in the extent of energy transfer for either the Tn–Tm*–DAB-F-actin complex or the Tn–Tm*–TNP-F-actin complex (Table II). This is surprising since based on structural studies we can expect Tm to move some 10–15 Å with respect to the grooves of actin. We considered the possibility that due to the presence of multiple actin-bound acceptors, the Tm movement may be such that no net change in the extent of energy transfer occurs. In order to test this possibility, we carried out a computer simulation study of this problem. The details of this study are presented in the Appendix; here, we briefly outline the methodology and summarize the conclusions. Using a model identical with that used by Parry & Squire (1973) in their simulation of X-ray diffraction studies, we systematically varied (1) the location of the donor attachment site along the length of Tm, (2) the location of the acceptor attachment site on the surface of an actin subunit, and (3) the position of Tm with respect to the grooves of the F-actin filament. The donor–acceptor distances were calculated, from which the energy transfer efficiencies, the values of τ_{da}, and the transfer efficiency were calculated. The results show that (1) the extent of energy transfer is not very dependent on the donor location along the length of Tm, (2) for a large majority of acceptor locations on actin, the extent of energy transfer is either considerably higher than what was observed or highly sensitive to Tm movement, and (3) there is, however, one region on the surface of actin that if the acceptor is located therein, the transfer efficiency is similar to that of our observed values *and* the extent of energy transfer is insensitive to Tm movement. This region is located on the outer surface of the actin filament (Figure 5b, crosses). It covers $\sim$10% of the surface of an actin subunit and extends from the top to the bottom of an actin subunit.

The foregoing discussion shows that our results may or may not be in conflict with results derived from structural studies, depending on the locations of the two acceptor-labeling sites. If either the Cys-373 or the nucleotide binding sites are located *outside* the aforementioned region on the surface of actin, then our failure to observe a calcium-dependent change in the extent of energy transfer excludes a calcium-induced movement of Tm. On the other hand, if the two sites are located within this region, then any movement of Tm cannot be detected by our method. Without independent information on the locations of the acceptor labeling sites these two possibilities cannot be resolved. Perhaps, when a high-resolution electron density map of actin (Suck et al., 1981) becomes available, the issue will become more clear. It is interesting to note that based on energy transfer measurements between successive subunits, Taylor et al. (1981) concluded that Cys-373 lies on the outer surface of the actin filament, in the same general region as that shown in Figure 5. A distance of 30 Å between the nucleotide binding site and Cys-373 of actin had been reported based on energy transfer measurements (Miki & Mihashi, 1978). Since our region extends from the top to the bottom of an actin subunit, and the diameter of the actin subunit is $\sim$48 Å, two sites separated by a distance of 30 Å can easily be accommodated within the region.

Our simulation study suggests interpretations of other workers' results. Consider the case that Tm does move in response to Ca^{2+} as suggested by structural studies. Then our results can be understood if both the DAB-labeling site (at Cys-373) and the TNP-ADP-labeling site (at the nucleotide binding site) in actin lie within the aforementioned region. In their work Lin & Dowben (1983) reported that the donor was attached to Cys-36 of $\alpha\beta$Tm, while the acceptor was attached to Cys-373 of actin. Since our simulation study showed that the extent of energy transfer is not very dependent on the location of the donor along the length of Tm, their finding of no calcium-dependent change in the extent of energy transfer is consistent with our analysis. Also, in their work, Poo & Hartshorne (1976) used reagents that could label lysine res-

idues at a variety of sites. It is possible that some of the acceptor-labeling sites were located outside this region and give rise to their observed calcium sensitivity in the extent of energy transfer. Our analysis also suggests that future work on this problem should be directed toward seeking additional acceptor-labeling sites in actin. We are currently carrying out such studies that utilize a nonspecific reagent as possible multiple acceptors on actin and the same AEDANS label attached to Cys-190 of Tm as the donor.

Acknowledgments

We thank Drs. Enoch Small and Irvin Isenberg for making available to us their FLUOR program for three-exponential method of moments analysis. We thank Dr. John Gergely for critically reviewing the manuscript.

References

Bender, N., Fasold, H., Kenmoku, A., Middelhoff, G., & Volk, K. (1976) *Eur. J. Biochem. 64*, 215–218.
Bridgen, J. (1972) *Biochem. J. 126*, 21–25.
Dale, R. E., & Eisinger, J. (1975) *Biochemical Fluorescence: Concepts* (Chen, R. F., & Edelhoch, H., Eds.) Vol. I, pp 115–284, Marcel Dekker, New York.
Ebashi, S., & Endo, M. (1968) *Prog. Biophys. Mol. Biol. 18*, 123–183.
Elzinga, M., & Collins, J. H. (1975) *J. Biol. Chem. 250*, 5897–5905.
Elzinga, M., Collins, J. H., Kuehl, W. M., & Adelstein, R. (1973) *Proc. Natl. Acad. Sci. U.S.A. 70*, 2687–2691.
Fairclough, R. H., & Cantor, C. R. (1978) *Methods Enzymol. 28*, 347–379.
Forster, T. (1959) *Discuss. Faraday Soc. 27*, 7–17.
Gillis, J. M., & O'Brien, E. J. (1975) *J. Mol. Biol. 99*, 445–459.
Haselgrove, J. (1972) *Cold Spring Harbor Symp. Quant. Biol. 37*, 341–352.
Hiratsuka, T., & Uchida, K. (1973) *Biochim. Biophys. Acta 320*, 635–647.
Hudson, E. N., & Weber, G. (1973) *Biochemistry 15*, 4154–4161.
Huxley, H. E. (1971) *Biochem. J. 125*, 85p.
Huxley, H. E. (1972) *Cold Spring Harbor Symp. Quant. Biol. 37*, 361–376.
Kawato, S., Kinosita, K., & Ikegami, A. (1977) *Biochemistry 16*, 2319–2324.
Lamkin, M., Tao, T., & Lehrer, S. S. (1983) *Biochemistry* (preceding paper in this issue).
Lehrer, S. S., & Kerwar, G. (1972) *Biochemistry 11*, 1211–1216.
Lehrer, S. S., Nagy, B., & Gergely, J. (1972) *Arch. Biochem. Biophys. 150*, 164–174.
Lin, T.-I. (1978) *Arch. Biochem. Biophys. 185*, 285–300.
Lin, T.-I., & Dowben, R. M. (1983) *J. Biol. Chem. 258*, 5142–5150.
Lusty, C. J., & Fasold, H. (1969) *Biochemistry 8*, 2933–2939.
Miki, M., & Mihashi, K. (1978) *Biochim. Biophys. Acta 533*, 163–172.
Parry, D. A. D., & Squire, J. M. (1973) *J. Mol. Biol. 75*, 33–55.
Poo, W.-J., & Hartshorne, D. J. (1976) *Biochem. Biophys. Res. Commun. 70*, 406–412.
Scott, T. G., Spencer, R. D., Leonard, N. J., & Weber, G. (1970) *J. Am. Chem. Soc. 92*, 687.
Stryer, L. (1978) *Annu. Rev. Biochem. 47*, 819–846.
Suck, D., Kabsch, W., & Mannherz, H. G. (1981) *Proc. Natl. Acad. Sci. U.S.A. 78*, 4319–4323.
Tao, T. (1978) *FEBS Lett. 93*, 146–149.
Tao, T., & Cho, J. (1979) *Biochemistry 18*, 2759–2765.
Taylor, D. L., Reidler, J., Spudich, J. A., & Stryer, L. (1981) *J. Cell Biol. 89*, 362–367.
Vibert, P. J., Haselgrove, J. C., Lowy, J., & Poulsen, F. R. (1972) *J. Mol. Biol. 71*, 757–767.
Wahl, P., Tawada, K., & Auchet, J.-C. (1978) *Eur. J. Biochem. 88*, 421–424.
Wakabayashi, T., Huxley, H. E., Amos, L. A., & Klug, A. (1975) *J. Mol. Biol. 93*, 477–497.
Wu, C.-W., Yarbrough, L. R., Wu, F. Y.-H., & Hillel, Z. (1976) *Biochemistry 15*, 2097.

Appendix: Computer Simulation Study on the Extent of Energy Transfer from a Single Tm-Bound Donor to Multiple Actin-Bound Acceptors

The purpose of this study is to ascertain whether it is possible for the Tm-bound donor and the actin-bound acceptors to be so located relative to each other that the movement of Tm with respect to the grooves of actin produces no net change in the extent of energy transfer. The model that we adopted is identical with what Parry & Squire (1973) used to simulate X-ray diffraction studies. F-actin was modeled as a single start 13_6 helix, composed of spherical subunits of radii 24 Å. The subunits are centered at a distance of 24 Å from the helix axis, with a vertical displacement of 27.3 Å between successive subunits. Tm was modeled as a continuous strand lying along the length of the actin filament. A computer program was written that systematically varied three parameters (1) The first parameter was the position of Tm in the actin grooves. This is defined by the angle ϕ_t (Figure 4a). Given ϕ_t, the distance r_t from the actin helix axis to the center of Tm (Figure 4a) is fixed and had been calculated by Parry & Squire (1973). (2) The second parameter was the location of the donor along the length of Tm. The symmetry of the actin helix is such that the scan needed only be carried out over the rise of one actin subunit, viz., 27.3 Å. The donor was assumed to be located at the center of the Tm strand. (3) The third parameter was the location of the acceptor on the surface of actin. This is defined by the angular variables θ_a and ϕ_a (Figure 5a). Once the location of an acceptor on one actin subunit was fixed, the locations of the acceptors on all the other actin subunits along the filament were generated according to the actin helix parameters. For each selection of the three parameters, the distances R_i between the Tm-bound donor and each actin-bound acceptor were then calculated. From these distances, k_t, the total energy transfer rate, and τ_{da}, the donor lifetime in the presence of acceptors, were calculated by using the following equations:

$$k_t = (1/\tau_d)\sum_i (R_0/R_i)^6 \quad (3)$$

$$1/\tau_{da} = 1/\tau_d + k_t \quad (4)$$

where R_0 is the donor–acceptor critical transfer distance, here taken to be 40 Å, and τ_d is the donor lifetime in the absence of acceptors, here taken to be 13.55 ns. Note that implicit in taking R_0 to be 40 Å lies the assumption that the orientation factor κ^2 takes on the same value of $^2/_3$ for all donor–acceptor pairs. This is justified by the fact that the donor on Tm and possibly the acceptor on actin possess considerable rotational freedom, such that κ^2 dynamically averages to nearly $^2/_3$ for all donor–acceptor pairs. We have chosen to monitor the variations in τ_{da} because it is the most direct experimental observable; τ_{da} can vary between 0 and 13.55 ns, corresponding to infinitely high extent of energy transfer and no energy

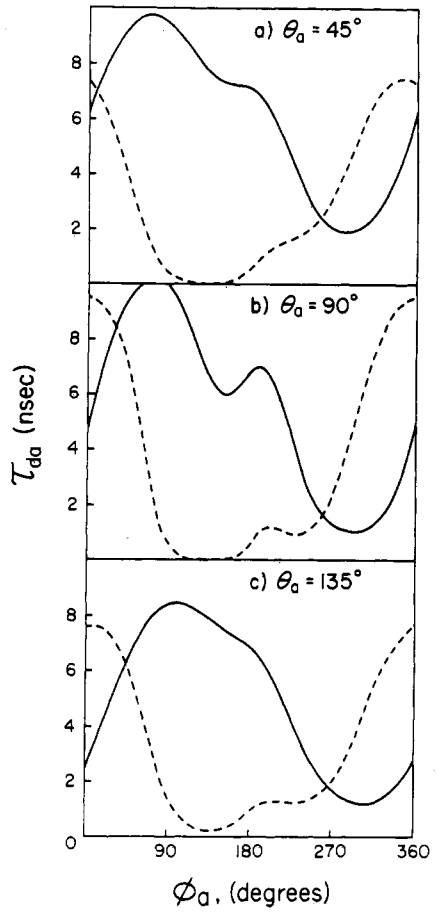

FIGURE 3: Calculated variation in τ_{da} with respect to acceptor location on the surface of an actin subunit. θ_a and ϕ_a are the polar and azimuthal angles that define the acceptor location (Figure 5a). The donor is fixed at the same vertical height as one of the actin-bound acceptors (i.e., $\Delta z = 0$). The solid line is τ_{da1} or τ_{da} obtained when Tm is positioned in the center of the actin groove ($\phi_t = 90°$). The broken line is τ_{da2} or τ_{da} obtained when Tm is half-way out of the actin groove ($\phi_t = 45°$).

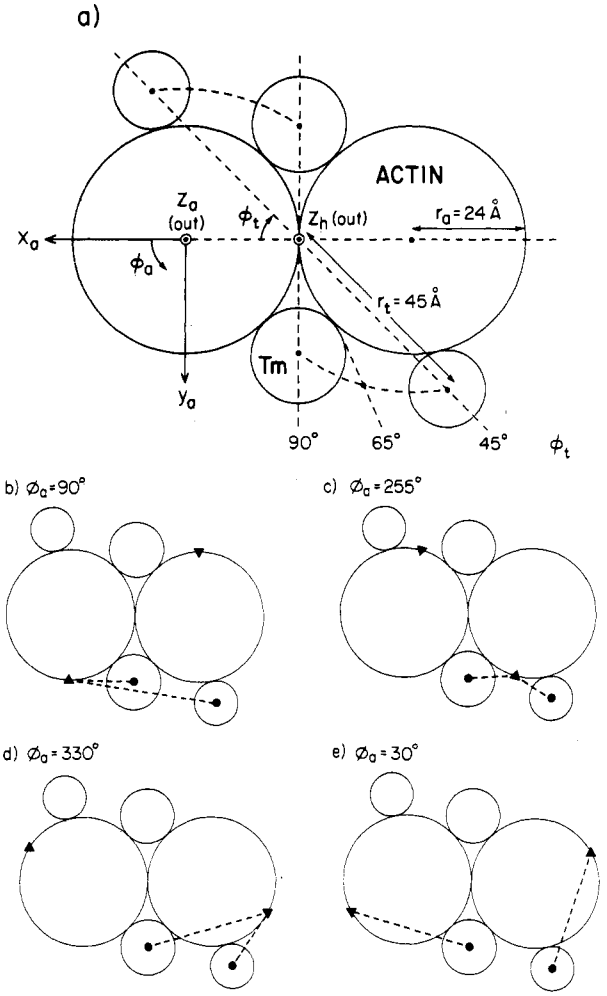

FIGURE 4: (a) Helical projection of the model for the Tm–F-actin complex [taken largely from Parry & Squire (1973)]. z_h is the actin helix axis; actin subunits are assumed to be spheres of radii $r_a = 24$ Å, centered at 24 Å from z_h. x_a, y_a, and z_a are actin-fixed axes that define the acceptor locations on actin (see also Figure 5a). The position of Tm with respect to the actin groove is defined by ϕ_t. Given ϕ_t, the distance r_t from the helix axis to the center of Tm is fixed by the geometry and had been calculated by Parry & Squire (1973). (b) How the extent of energy transfer varies with the position of Tm strongly depends on the azimuthal angle (ϕ_a) of the acceptor location. In these diagrams, the solid triangles represent the acceptors, and the solid circles represent the donors. For $\phi_a = 90°$, the donor is moderately near an acceptor when Tm is in the center of the actin groove ($\phi_t = 90°$). As Tm moves out of the groove (ϕ_t approaches 45°) the donor moves away from that acceptor, giving rise to a decrease in the extent of energy transfer and an increase in the magnitude of τ_{da} (the donor lifetime in the presence of the acceptor). (c) For $\phi_a = 255°$, the acceptor is near the donor regardless of the Tm position. Considerable energy transfer occurs, yielding low values of τ_{da} at all values of ϕ_t. (d) For $\phi_a = 330°$, the donor moves closer toward the acceptor as Tm moves out of the active groove. The extent of energy transfer increases, while τ_{da} decreases as ϕ_t varies from 90° to 45°. (e) For $\phi_a = 30°$, the donor moves from the vicinity of one acceptor to the vicinity of another acceptor as Tm moves out of the actin groove. A moderate extent of energy transfer occurs, yielding moderately high values of τ_{da} at all values of ϕ_t.

transfer, respectively. The sum in eq 3 was carried over 11 actin subunits. Because the energy transfer rate drops off as the inverse sixth power of the distance, acceptors bound to actin subunits at either end of the summation contribute very little to the total transfer rate.

This study yielded the following results: As illustrated in Table III, τ_{da} is not very sensitive to the location of the donor along the length of Tm. In contrast, τ_{da} is highly sensitive to the acceptor location on actin, the dependence being stronger with the azimuthal angle ϕ_a than with the polar angle θ_a. The dependence on ϕ_a is such that characteristic minima occur when the acceptor is near a Tm-bound donor, while maxima occur when no donor is nearby. As an example, suppose that θ_a is fixed at 90° and ϕ_t is fixed at 90° (corresponding to Tm positioned at the center of the actin groove), then, as ϕ_a increases, a minimum is attained at $\phi_a = 135°$ when the acceptor approaches a donor bound to one Tm strand and again at $\phi_a = 230°$ when the acceptor approaches a donor bound to the opposite Tm strand (Figure 3b; see also diagram in Figure 4b). At $\phi_a = 0°$, a maximum occurs when the acceptor is farthest away from either donor. Varying the polar angle θ_a causes the positions of the minima and maxima to shift slightly, but the general features of the periodicity are preserved (Figure 3).

How τ_{da} varies with Tm position depends on where the acceptor is located. Table IV illustrates that as Tm moves away from the center of the actin groove (ϕ_t decreases 90° to 45°), τ_{da} can increase from 0.6 to 10.0 ns or remain roughly constant at 8–10 ns for two different acceptor locations. From Figure 3, and described diagramatically in Figure 4b–e, we deduced that four situations arise: (1) For $\phi_a \simeq 90°$, τ_{da} increases sharply from ~1 to ~10 ns as Tm moves away from the center of the actin groove. (2) For $\phi_a \simeq 255°$, τ_{da} remains nearly constant at ~2 ns irrespective of Tm position. (3) For $\phi_a \simeq 330°$, τ_{da} decreases from ~8 to ~2 ns as Tm moves out

Table III: Variation of τ_{da} with Vertical Displacement of the Donor along the Length of Tm[a]

	$\theta_a = 90°, \phi_a = 90°$		$\theta_a = 90°, \phi_a = 255°$		$\theta_a = 90°, \phi_a = 330°$		$\theta_a = 90°, \phi_a = 30°$	
Δz (Å)	τ_{da1} (ns)	τ_{da2} (ns)	τ_{da1} (ns)	τ_{da2} (ns)	τ_{da1} (ns)	τ_{da2} (ns)	τ_{da1} (ns)	τ_{da2} (ns)
14	0.77	9.75	0.21	0.41	8.11	0.44	8.12	7.77
7	0.53	9.80	0.62	1.25	8.34	0.86	8.12	7.89
0	0.59	9.95	1.50	1.79	8.68	1.92	8.36	8.36
−7	1.02	10.10	1.56	0.85	8.93	3.02	8.70	8.90
−14	1.95	10.16	0.67	0.25	8.93	2.33	8.94	9.16

[a] θ_a and ϕ_a are the polar and azimuthal angles that define the acceptor locations on the surface of an actin subunit (Figure 5). τ_{da1} and τ_{da2} are τ_{da}'s obtained when Tm is positioned at $\phi_t = 90°$ and 45°, respectively (Figure 4a). Δz is the vertical displacement of the donor with respect to the acceptor on an actin subunit. Note that neither τ_{da1} nor τ_{da2} is very sensitive to variations in Δz.

Table IV: Variation of τ_{da} and Donor–Acceptor Distances with the Position of Tm[a]

			R_i (Å) at i =						
θ_a (deg)	ϕ_a (deg)	ϕ_t (deg)	−2	−1	0	+1	+2	R' (Å)	τ_{da} (ns)
90	90	90	65.2	58.3	24.0	63.0	56.0	23.9	0.59
90	90	75	70.8	58.7	32.6	65.7	57.6	32.1	2.85
90	90	60	77.8	57.6	43.3	66.9	61.6	40.7	7.14
90	90	45	87.0	56.5	56.4	68.2	68.8	47.5	9.95
90	30	90	79.2	59.7	46.6	68.1	64.7	43.4	8.36
90	30	75	86.2	56.3	55.8	67.4	69.0	47.2	9.84
90	30	60	93.9	51.1	66.4	64.8	75.8	47.0	9.80
90	30	45	103.4	45.0	79.1	61.3	85.6	43.4	8.36

[a] θ_a and ϕ_a were defined in footnote *a* of Table III. ϕ_t is the azimuthal angle that defines the position of Tm with respect to the actin groove (Figure 4a). R_i's are distances from the donor to acceptors on successive actin subunits. R' is the apparent distance calculated on the assumption that only one acceptor was present. τ_{da} is the calculated donor lifetime in the presence of acceptors. $\Delta z = 0$ for these calculations. Note that $R' \leq R$, where R is the distance between the donor and the nearest acceptor(s) (underscored). If only one acceptor is near the donor, then $R' \simeq R$; if n acceptors are near, then $R' \simeq n^{1/6}R$.

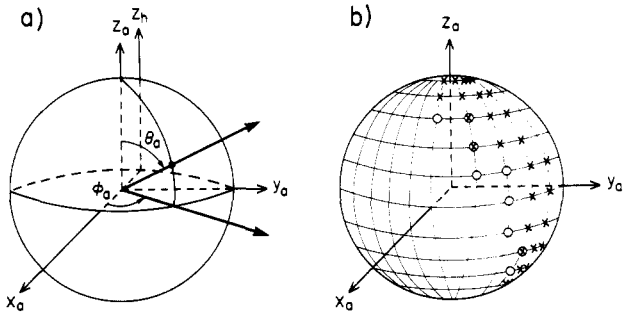

FIGURE 5: (a) x_a, y_a, and z_a are axes that define the location of the acceptor on the surface of an actin subunit. The origin is at the center of the actin subunit, which is assumed to be spherical. z_h is the axis of the F-actin helix. θ_a is the polar angular coordinate, and ϕ_a is the azimuthal angular coordinate. (b) Acceptor locations that can give rise to the experimental observations. A computer program searches for all acceptor locations on the surface of actin that give rise to two conditions simultaneously: (1) Both τ_{da1} and τ_{da2} (values of τ_{da} corresponding to $\phi_t = 90°$ and 45°, respectively) exceed or equal 6.00 ns. (2) τ_{da1} and τ_{da2} do not differ by more than 1.5 ns. The procedure yielded the open circles. The crosses were obtained when τ_{da1} and τ_{da2} were values of τ_{da} corresponding to $\phi_t = 65°$ and 45°, respectively.

of the active groove. (4) For $\phi_a \simeq 30°$, τ_{da} remains roughly constant at ~8 ns.

Of the four situations described above, only the last one ($\phi_a \simeq 30°$) resembles the experimental observations with respect to both the extent of energy transfer and its insensitivity to Tm movement. Figure 4e depicts how this occurs: when Tm is positioned at the center of the groove, the donor is moderately near an acceptor bound to one of the actin subunits. As Tm moves out of the groove the donor moves away from that acceptor but approaches another acceptor bound to a subunit in the opposite strand of the actin double helix. A search was made for all acceptor locations on actin that give rise to two conditions simultaneously: (1) The calculated τ_{da} is nearly the observed τ_{da}, viz., 6 ns or greater. (2) Shifting the position of Tm from one extreme of being in the center of the actin groove ($\phi_t = 90°$) to the other extreme of half-way out of the groove ($\phi_t = 45°$) causes a change of no more than 1.5 ns in τ_{da} (1.5 ns being the estimated uncertainty in the experimentally measured τ_{da}). The results show that such acceptor locations are restricted in a narrow area defined by ϕ_a = 0–45° and θ_a = 45–135° (Figure 5b, open circles). Neither the size nor the location of this area varied much when the donor location along the length of Tm was varied. The actual X-ray diffraction results suggest that the movement of Tm is such that ϕ_t varies only from 65° to 45° (Parry & Squire, 1973). Inserting this condition to the search procedure yielded an area that was expanded in size but one that was nevertheless confined within ϕ_a = 0–90° (Figure 5b, crosses).

In conclusion, our simulation study shows that if an acceptor is located within the region shown in Figure 5b, then the movement of Tm would produce no net change in the energy transfer efficiency. Thus, our experimental observation of no calcium-dependent change in energy transfer efficiency may or may not be in conflict with the notion of a Tm movement, depending on whether the two acceptors sites are located outside or within the aforementioned region.